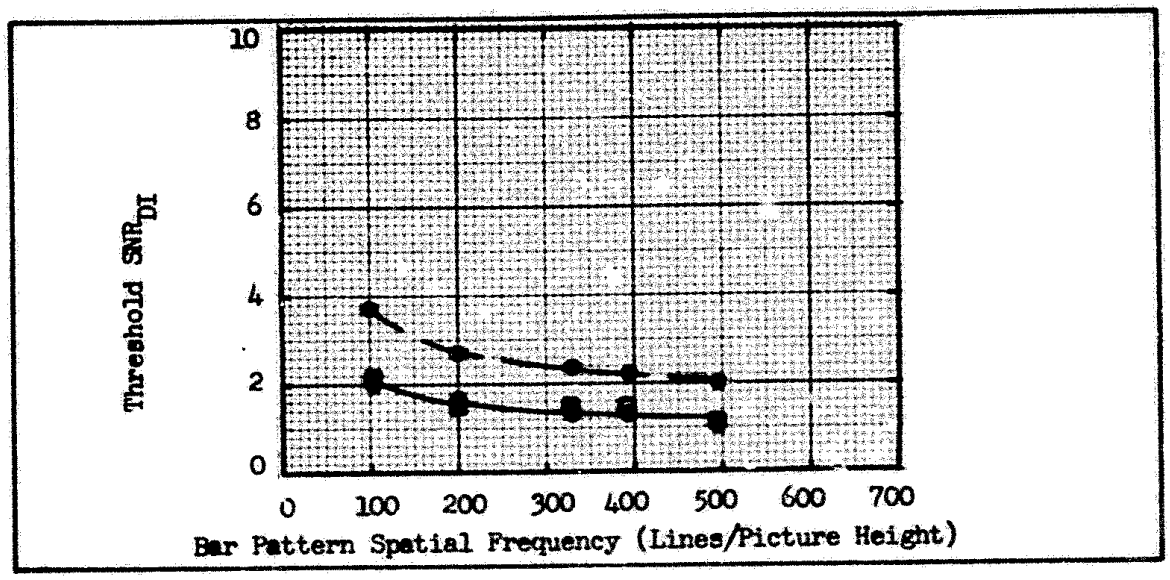

Fig. 79 Exp. No. 1 and 2. Threshold SNR_{DI} for ● Original Data and Present Data ○ Minimum Illumination Background □ 1 ft-Lambert Background - Constant Aspect Pattern Case A MTF

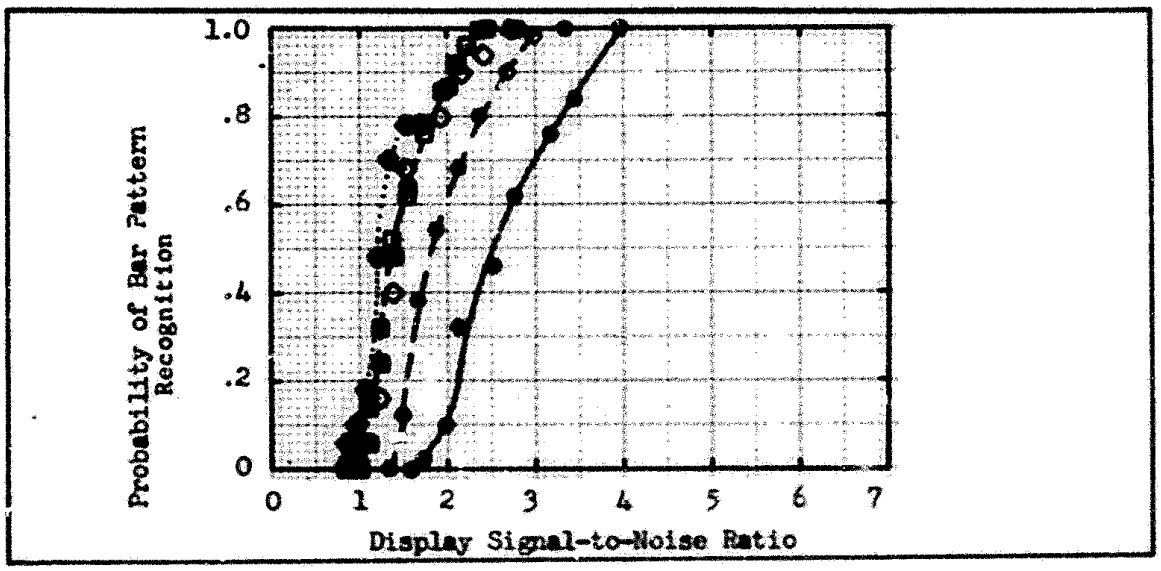

Fig.80 Exp. No. 2 Probability of Bar Pattern Recognition Versus Display Signal to Noise Ratio for Case A MTF, 1 ft-Lambert Monitor and 1 ft-Lambert Background Bar Pattern Spatial Frequency ○ 104, ● 200, □ 329, ■ 396, ◇ 482, ◆ 635 AF 5 Bar

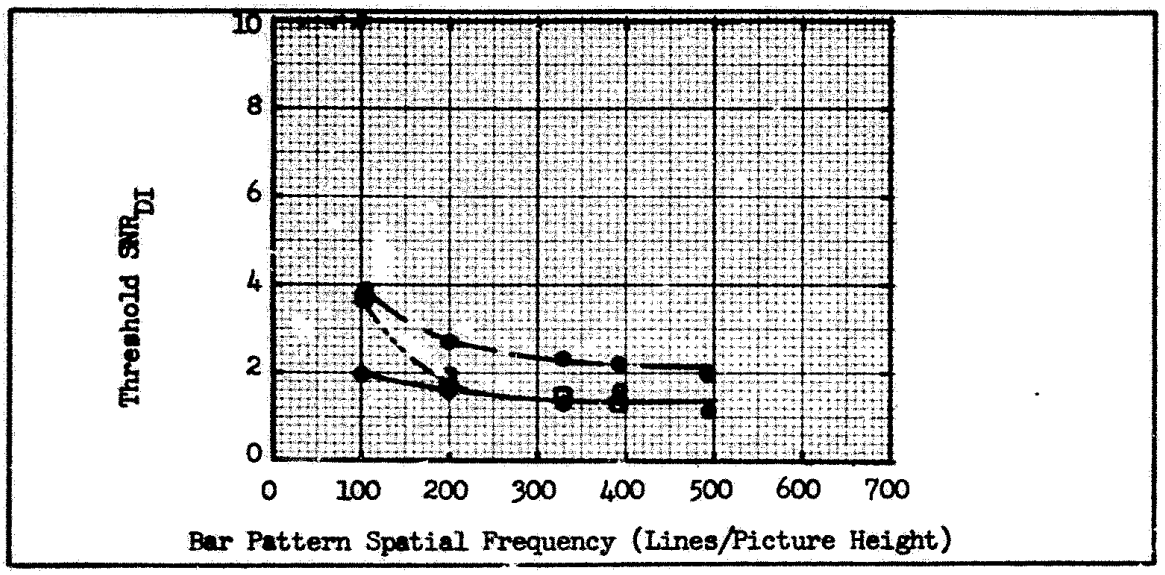

Fig. 81 Exp. No. 3. Threshold SNR_{DI} for ● Original Data and Present Data 1 ft.-Lambert Background ○ Normal □ Very Critical Threshold Judgment - Constant Aspect Pattern Case A MTF

the square data points, □ . As can be seen from a comparison of the squares and open circle of Fig. 79, the effect of the surrounding brightness was negligible but, again lower threshold values of SNR_{DI} were obtained than were obtained on the previous program.

After carefully checking the experimental set-up, recalibrating meters and oscilloscopes, checking terminations, lens focus, camera MTF, and signal currents, a third experiment was performed with one observer in which an attempt was made to be much more critical in establishing the criteria for resolving or not resolving of the bar pattern. The background was at 1 ft. Lambert. The threshold SNR_D results are shown in Fig. 81 by the square data points and then for experiment #1, by the open circles and, again for comparison, the original data from Ref. (2) is shown by solid circles. It was hypothesized that a more critical criteria for bar pattern

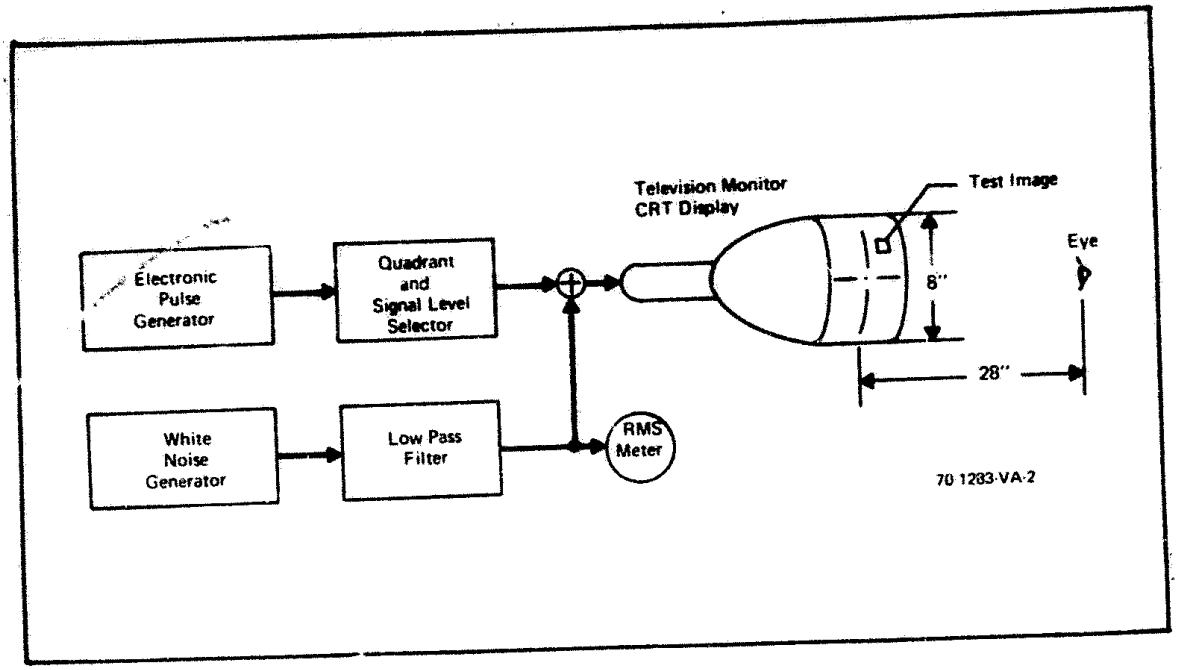

Fig. 82 The Display Signal-to-Noise Ratio Experiment

recognition would correspond with increased SNR_{DI} values and indeed, as is seen in Fig. 81 at low line numbers, this hypothesis is born out. However, virtually no change is observed at higher line numbers. A conscious change in the threshold does not account for the change in the experimental results. Why then are the present results different?

For both of the present experiments and the previous ones a more or less constant pool of about 10 people were used. All of these people were involved in numerous other resolution experiments between the old program and the new and it is postulated that the difference in the curves reflect the learning curves of the subjects. Time did not permit rerunning of the experiments with untrained subjects.

As a final check of the calibration of our equipment, an experiment was run using the set-up shown in Fig. 82. The set-up involved replacing

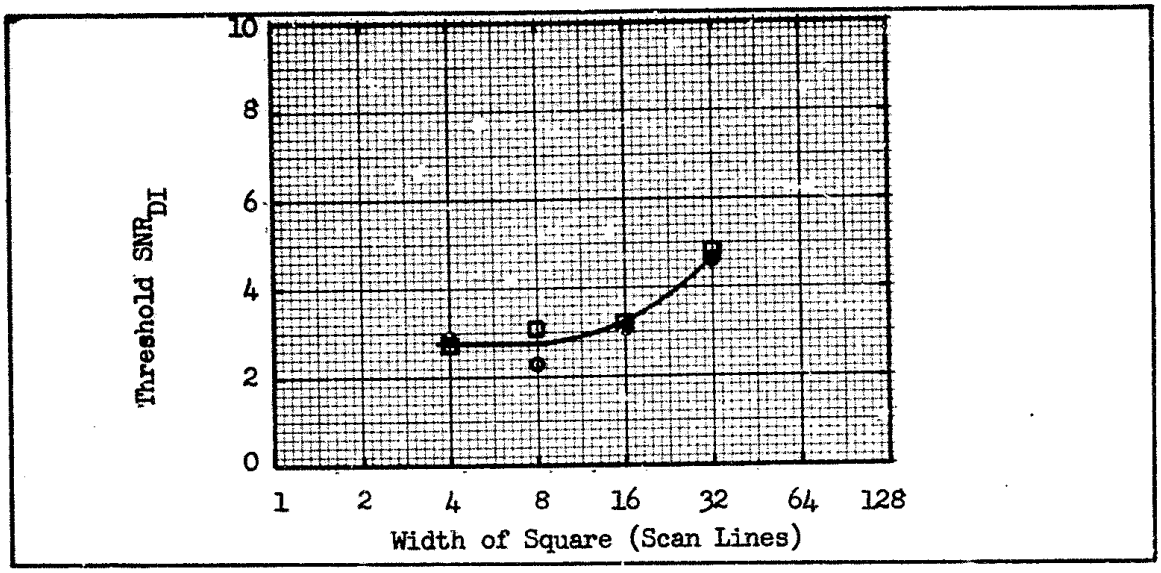

Fig. 83 Exp. No. 4. Threshold SNR_{DI} for Electronically Generated Squares o New Data □ Old Data

the vidicon by the electronic pulse generator and operating the monitor at the lower scan rate. The subject had to say in which quadrant of the display the electronically generated square was. Position, size, and SNR_D were randomly varied. In Fig. 83, the threshold values of SNR_{DI} as a function of square width (expressed in number of raster scan lines for convenience), is shown for the present experiment by the open circle points, o, and the results from the previous experiment [Ref. (2)], performed a year earlier by the open squares, □. No difference between the two results can be seen and it is concluded that the experimental set-up is correctly calibrated and that, most likely, the differences which were observed for the bar patterns recognition experiments were due to observer training.

Part of the problem with the bar pattern experiments is that there

was no way to judge the correctness of the observer's response. An observer said he could resolve a given pattern but this is highly subjective, and, apparently the criterion (be it unconscious) changed with training. For the detection of squares, we know if the subject was right or not and, indeed we can correct for random guesses. Bar pattern recognition could be made less subjective if an element of correctness/wrongness was introduced such as having a break in a bar and asking where the break was or maybe using different size Landalt C's with the position of the break randomly varied and again asking where the break was. Time did not permit testing of either of these hypotheses. A comparison of the new data discussed above and that which will be discussed below does show that a high degree of consistency exists for similar experiments and we believe that valid conclusions can be drawn from these experiments.

For the fifth experiment, set-up B for the MTF was used. Again the constant aspect pattern was utilized and in Fig. 84, the probability versus SNR_{DI} is plotted as a function of different spatial frequencies. In Fig. 85, the threshold SNR_{DI} values are plotted versus spatial frequency. A comparison Figs. 80 and 85 shows that nearly the same SNR_{DI} values are obtained for the two MTF cases with slightly closer agreement being obtained at the lower frequencies than at the higher frequencies. Finally, experiment six was performed with case C's MTF and the constant aspect pattern. Probability versus SNR_{DI} for this case is plotted in Fig. 86 and threshold SNR_{DI} versus spatial frequency is plotted in Fig. 87. Comparing Figs. 80 and 87, we see that again for low frequencies, the results are nearly the same for Case A and Case C MTF's but for higher frequencies, lower values of threshold SNR_{DI} is obtained for Case C than for Case A. The above

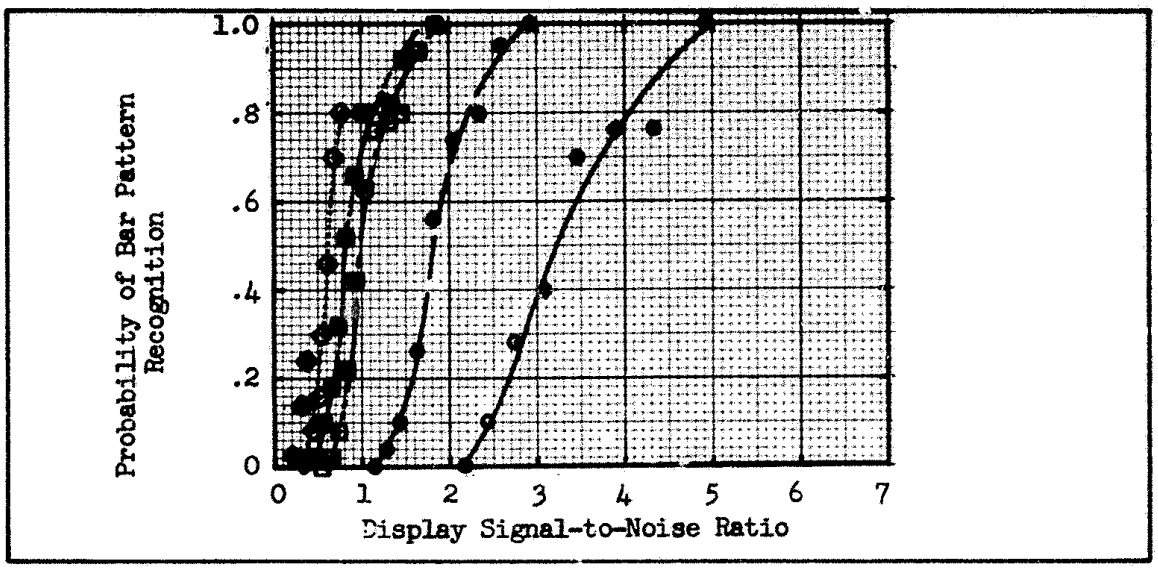

Fig. 84 Exp. No. 5. Probability of Bar Pattern Recognition-Constant Aspect Bars - Case B MTF Spatial Frequency ○ 104, ● 200, □ 329, ■ 396, ◇ 482, ◆ 635

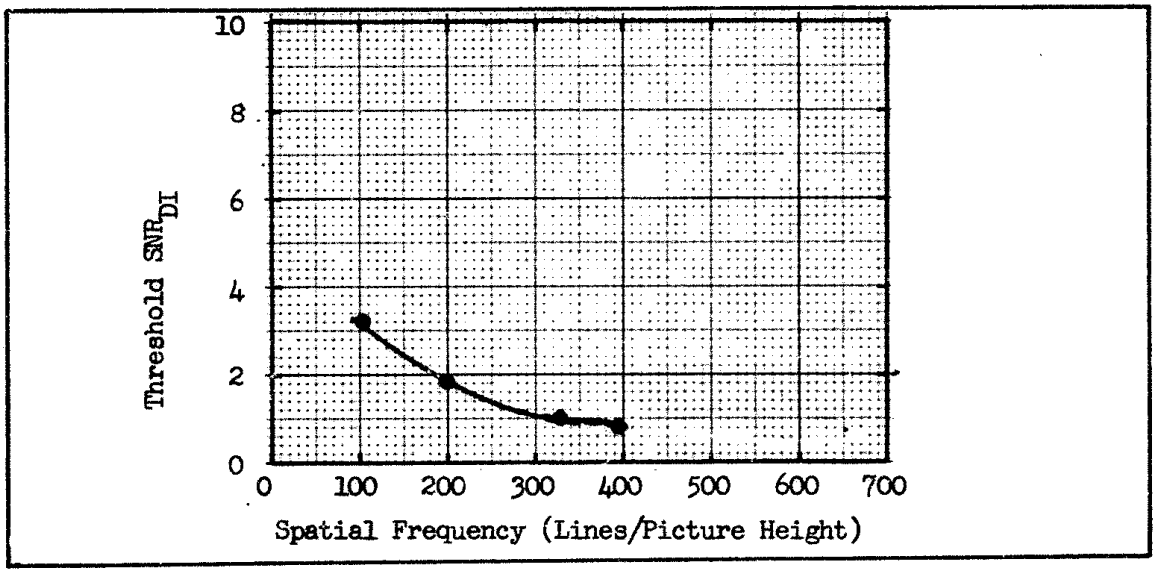

Fig. 85 Exp. No. 5. Threshold SNR_{DI} for Constant Aspect Bar Patterns Case B MTF

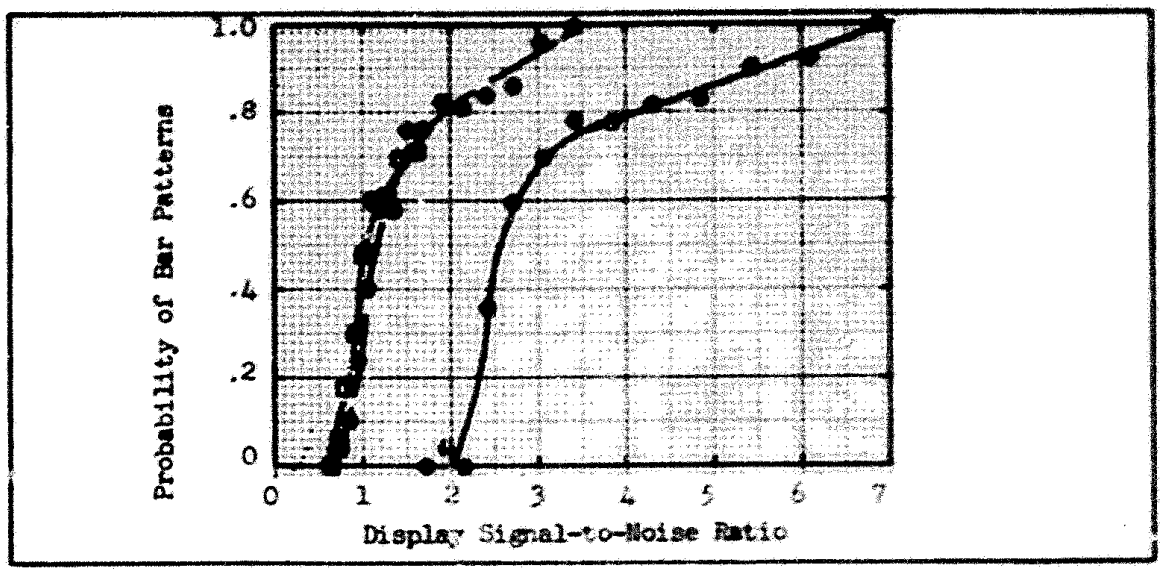

Fig. 86 Exp. No. 6. Probability of Bar Pattern Recognition for Case C, Constant Aspect Bar Patterns Spatial Frequency ○ 104, ● 200, □ 329

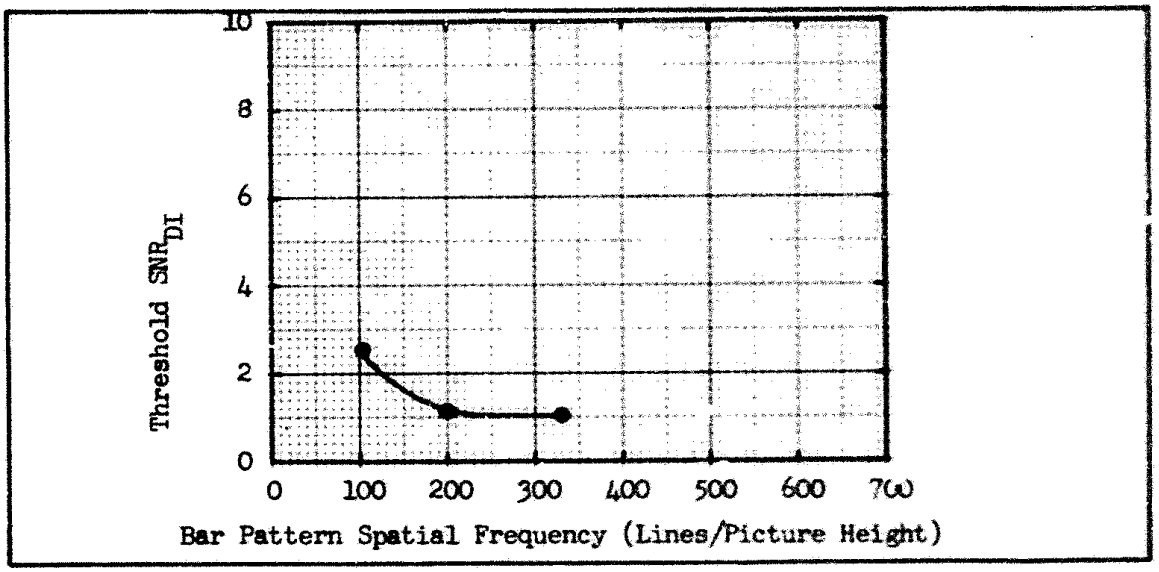

Fig. 87 Exp. No. 6. Threshold SNR_{DI} for Case C, Constant Aspect Pattern

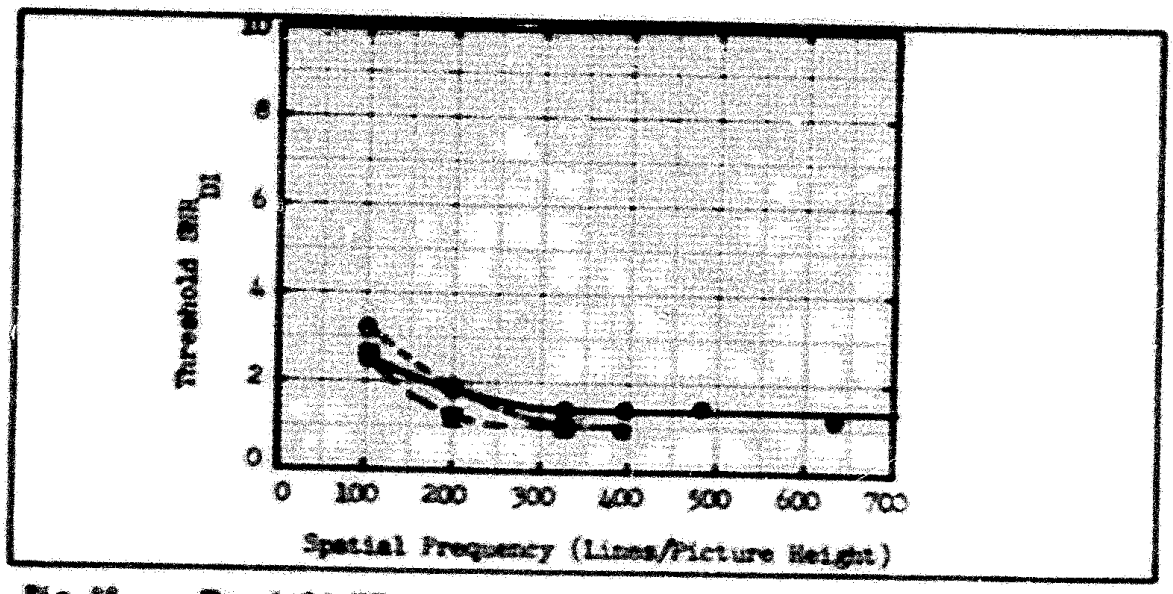

Fig. 88 Threshold SNR_{DI} for AF 5 Bar Pattern Case A ●, Case B ⊙, Case C ○ MTF's

results are summarized in Fig. 88 for the constant aspect patterns for Case A, B, and C MTF's. The values of SNR_{DI} are somewhat lower for Case B and C than A for higher spatial frequencies. One must be careful in concluding that lower SNR_{DI} values are obtained with poor MTF. Comparing the spread in the data at low frequencies where the experimental accuracy is the best shows a fairly large spread in the data so the difference is probably not very significant.

It must be also kept in mind that the calculation of SNR_D includes the MTF's effect on signal and on noise. For a given line number and SNR_D value, a much higher video signal-to-noise ratio is required for Case C MTF than for Case A MTF. The experimentally determined threshold values of SNR_D are somewhat lower for Case C's MTF than those for Case A's and as was mentioned the differences may be reflecting experimental error. More likely, we believe,

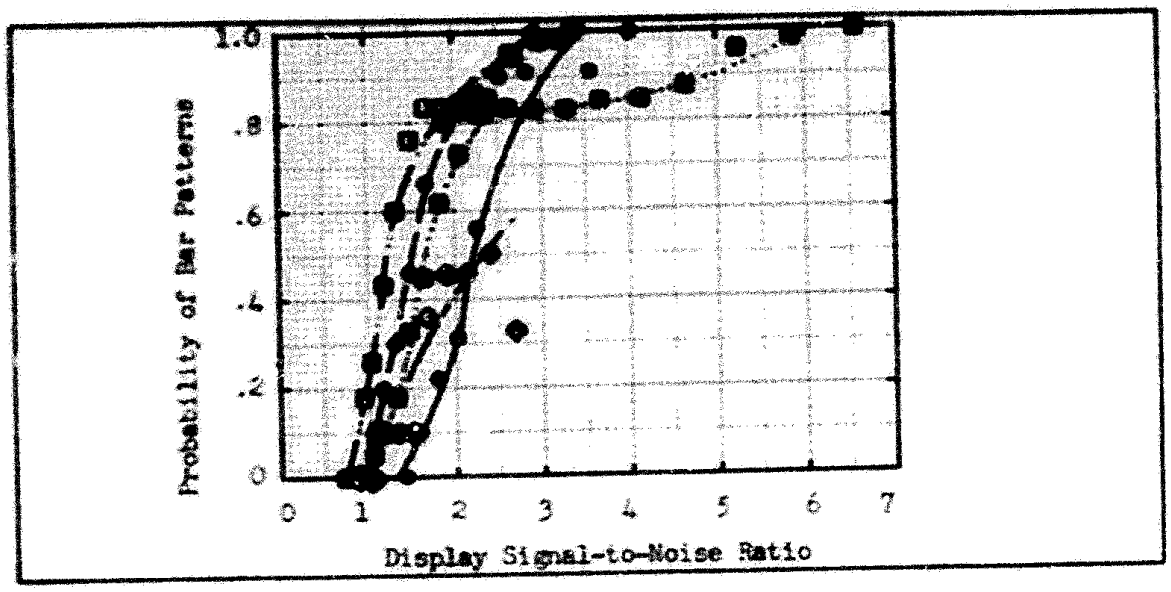

Fig. 89 Probability of Bar Pattern Recognition for Constant Length Bar Patterns - Case A MTF

is that for poor MTF's, our formulation for SNR_D is rather pessimistic, that is, the MTF's do not degrade the images detectability as much as theory would indicate. In any event, for the same broad area video signal-to-noise ratio, the better the MTF is, the more detectable the image is.

Experiment 7 used Case A MTF with the bar patterns of variable aspect and the experimental results are shown in Figs. 89 and 90. For comparison, the results with the constant aspect patterns are also shown in Fig. 90 and as is seen, the two cases are very similar for all but the highest line numbers.

Experiment 8 utilized the variable aspect pattern with Case C MTF and the threshold SNR_D vs spatial frequency curves for Case A and C are plotted in Fig. 91 . A somewhat lower result was obtained for Case C than for Case A.

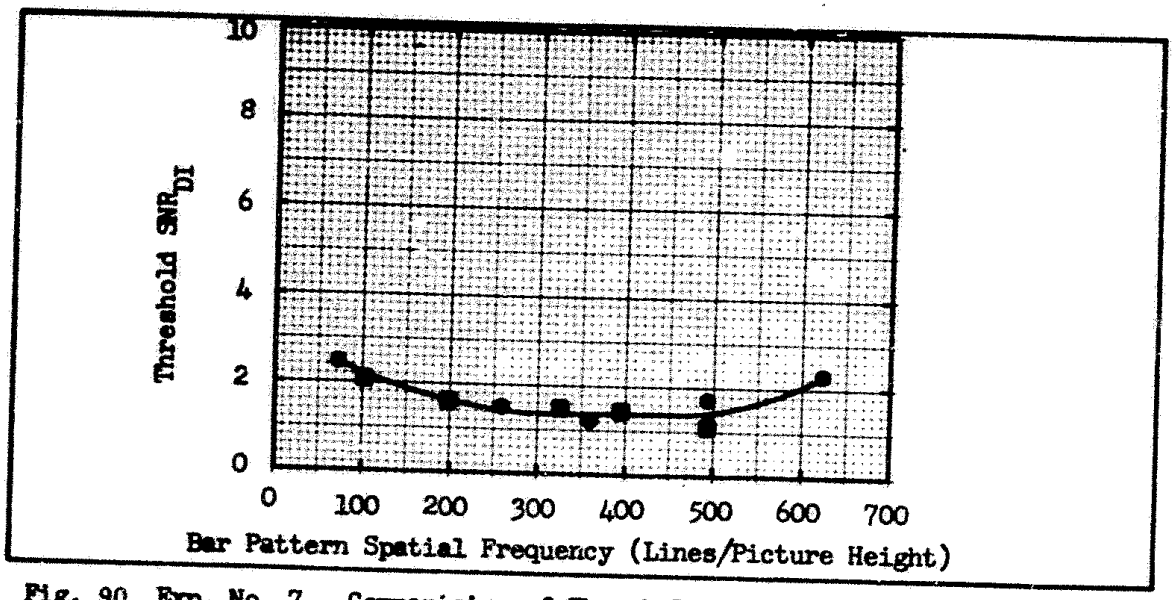

Fig. 90 Exp. No. 7. Comparision of Threshold SNR$_{DI}$ for Case A MTF, ● Constant Length, ■ Constant Aspect Bar Patterns

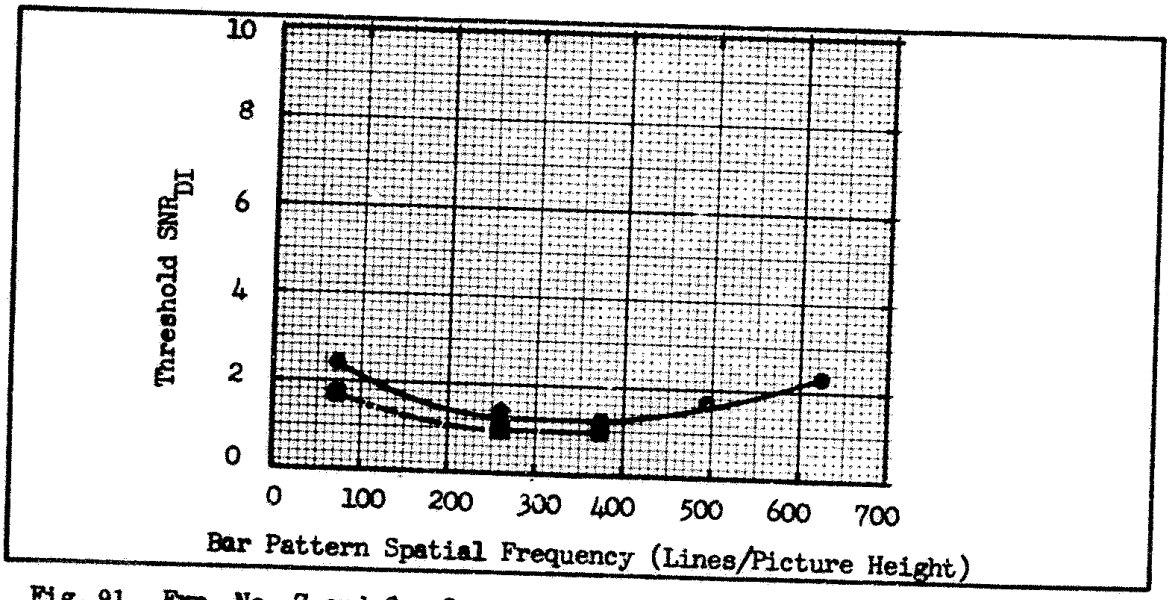

Fig. 91 Exp. No. 7 and 8. Comparison of Threshold SNR$_{DI}$ for Constant Length Bar Patterns Case A ○ , Case C □ MTF's

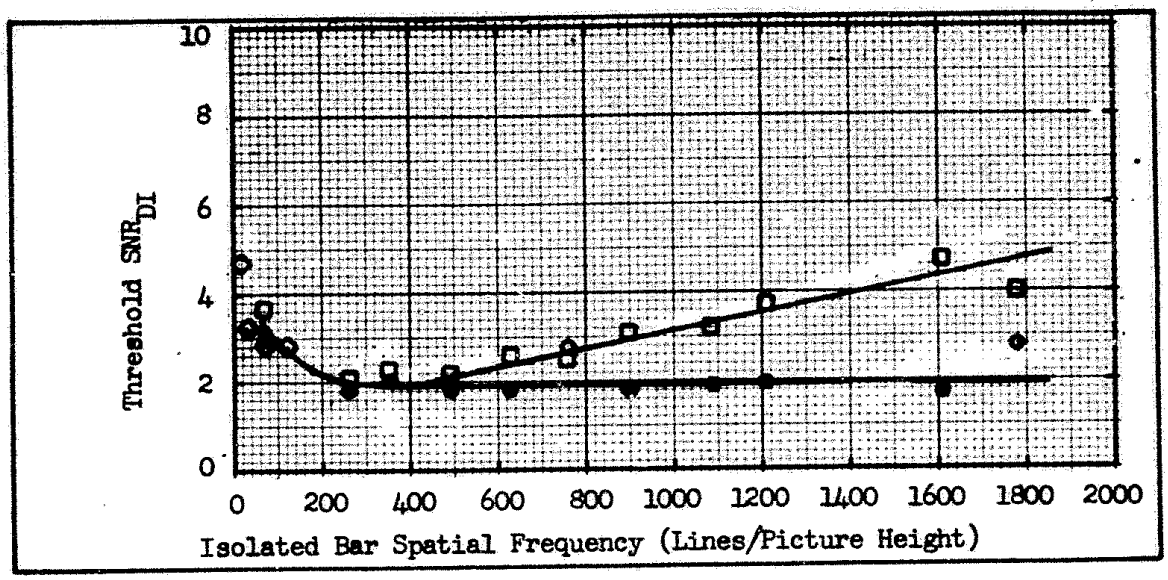

Fig. 92. Exp. No. 9 and 10, Threshold SNR_{DI} for Isolated Bars for Case A o , Case C □ MTF's, ◇ Electronically Generated Squares

The pattern with the isolated bars was used for the next two experiments, Case A MTF in experiment 9 and Case C MTF in experiment 10. The threshold SNR_{DI} versus spatial frequency plots for the two cases is shown in Fig. 92. The data is virtually the same up to a spatial frequency of about 500 lines/ picture height and then the data for Case C rises at a nearly constant rate. A rise in the threshold curve for Case A MTF is suggested at very high line numbers, N = 1780. A comparison of the data from Fig.83 for the electronically generated squares and that for isolated bars of Fig. 92 shows that the two sets of data are similar at low line numbers, the Case A MTF data being nearly the same as that for the electronic generated squares. This of course is not a surprise. At low line number for Case A, aperture effects are minimized and the results should be similar to those measured for the electronically generated squares where aperture effects are

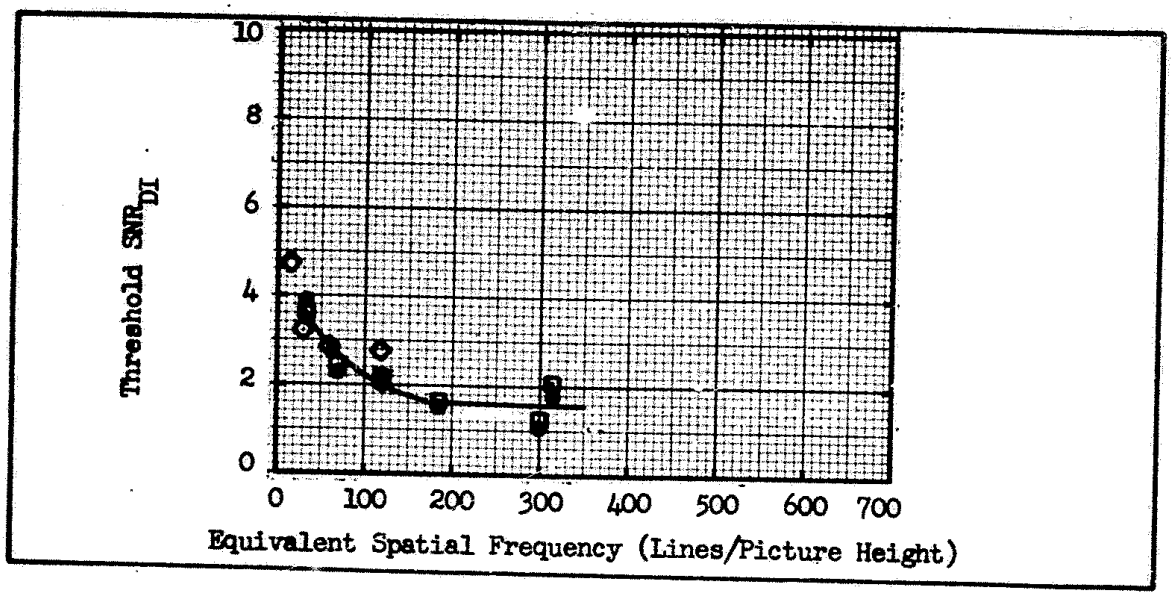

Fig. 93 Exp. No. 11 and 12. Threshold SNR_{DI} for Isolated Circles for Case A ○ , Case C □ MTF's, ◇ Electronically Generated Squares

negligible. This is further evidence that the present experimental set-up is functioning correctly.

The pattern with the isolated circles was also used with Case A MTF and Case C MTF and the threshold SNR_{DT} is plotted versus spatial frequency for the two cases in Fig. 93. Again, it is found that the data is consistent with that measured with the aperture free, electronic-target generator.

For aperiodic targets, from the comparison of the experiments with isolated bars and circles and those of the aperture free squares, it is seen that the theory as given by Eqs. (164) and (165) is confirmed, within experimental accuracy, for MTF's that are quite different from one another (N_e = 252 for Case A and N_e = 69 for Case C). Furthermore, it is seen that for bar patterns, the theory as given by Eqs. (160), (161), (162), and (163),

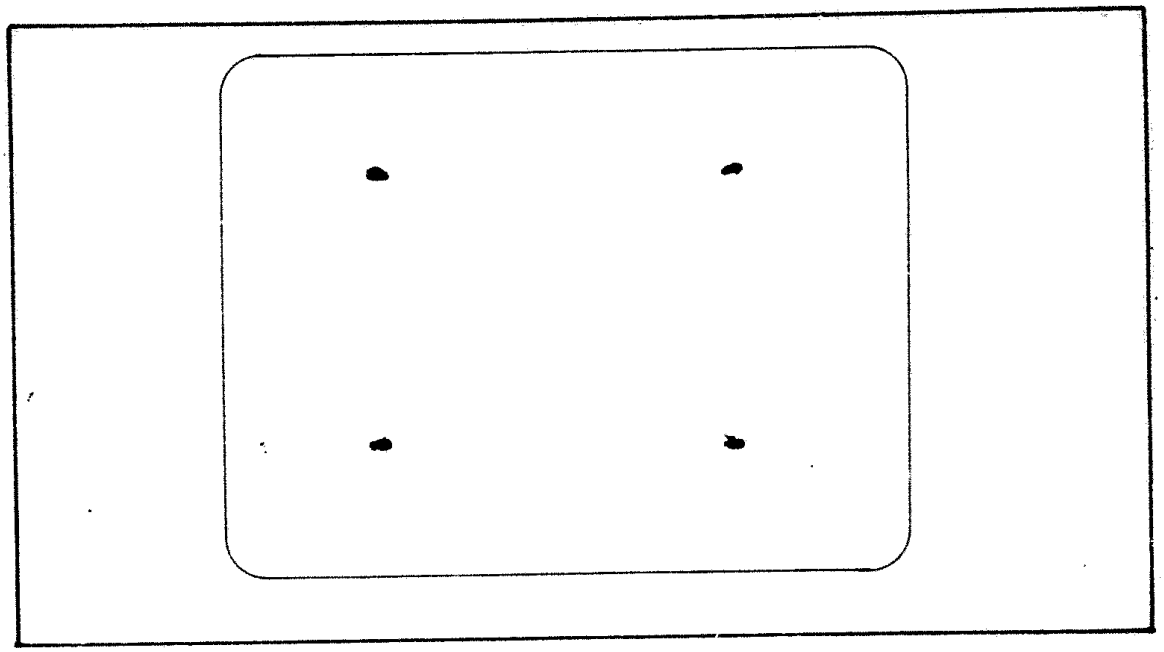

Fig. 94 Photographs of Models Used for Recognition Experiments - Upper Left, Tank; Upper Right, Van Truck; Lower Left, Half Track with Antenna; and Lower Right, Derrick Half Track.

gives a somewhat pessimistic result (smaller SNR_{DI}) for poor MTF's than it does for good MTF's. In effect, a system of poor MTF would actually perform somewhat better than the theory would suggest. The differences are in such a direction as to help the system designer.

Using the experimental set-up of Fig. 1, experiments were performed on tactical target recognitions using Case A and Case C to establish the impact of MTF's on real target recognition. The transparencies which were used were made from high quality photographs of vehicles amid a uniform white background. The photographs were taken at a depression angle of 45° from the horizontal and perpendicular to the vehicle's longitudinal axis, i.e., the sides and tops of the vehicles were imaged as is shown in Fig. 94. The vehicles included a tank, a van truck, a half track with top-mounted radar antenna and a tracked bulldozer with derrick. The areas of the

various vehicles were approximately 0.057 in^2 on the 8" x 10.7" display and subtended angles of about 0.34° by 0.68° at the observer's eye. The vehicle types and video SNR were randomly varied; and the probabilities of recognition, corrected for change, were determined. The SNR_{DI}'s for the various images were calculated on the basis of the area of a bar whose length and width are equal to the length of the vehicle's image and the width of the vehicle's image divided by 8. This is in accord with the equivalent bar pattern concept discussed in AFAL-TR-72-229. We note, however, one difference between the calculations for the bar pattern and the vehicular image's SNR_{DI}. In the case of the vehicular image, the signal amplitude was measured from the background signal level which was approximately constant, to the peak object signal level. For the "equivalent bar patterns," the signal levels were measured in terms of the mean signal excursion within the bar pattern area in the periodic direction. Had the peak-to-peak excursions about the average signal within the vehicle area been used (when the object is imaged against a uniform background), the thresholds SNR_{DI} would have been somewhat lower.

These difficulties result from the necessity of defining an image area and a signal excursion in order to calculate an SNR_{DI} threshold. In this connection, we observe that the criterion for bar pattern recognition is that the observer must be able to discern a modulation within the bar pattern whereas for vehicle image recognition, the vehicle's outline must be discerned. This outline may have periodic features but is more likely to be aperiodic.

Specifically, the SNR_{DI} was calculated from

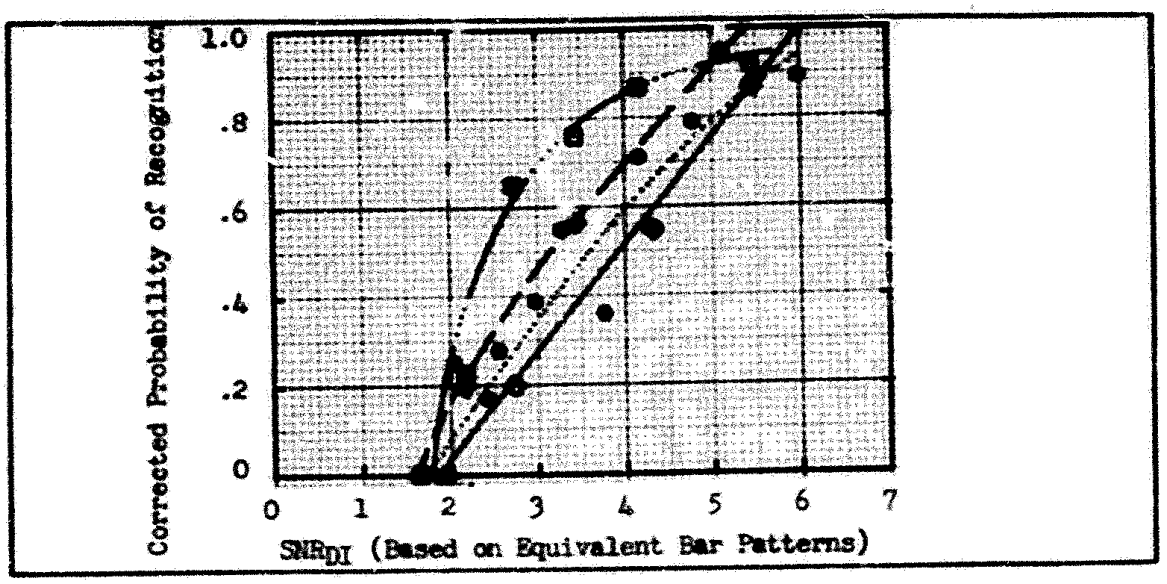

Fig. 95 Exp. No. 13. Tactical Target Recognition for Case A MTF
o Tank, ● Derrick, □ Truck, ◇ Radar Truck

$$SNR_{DI} = \left[2t\Delta f_V \frac{a}{8A}\right]^{\frac{1}{2}} SNR_V \tag{166}$$

where SNR_V was the largest zero to peak voltage in a frame of the image divided by the RMS value of the noise. The value of a/A that was used was the actual area of the image, a, on the transparency divided by the total area of the transparency, A, that was viewed. The factor of 8 in Eq. (166), comes from the assumption that we are to calculate SNR_{DI} on an equivalent bar pattern basis, that is, for recognition, one whose bars are each a/8 in area. In Figs. 95 and 96 , the probability versus SNR_{DI} is plotted for tactical target recognition for Case A and Case C, respectively. For Case A, the average threshold SNR_{DI} is 3.2 where as for Case C, the average threshold SNR_{DI} is 4.3 ; a value that is 34% higher than that for Case A.

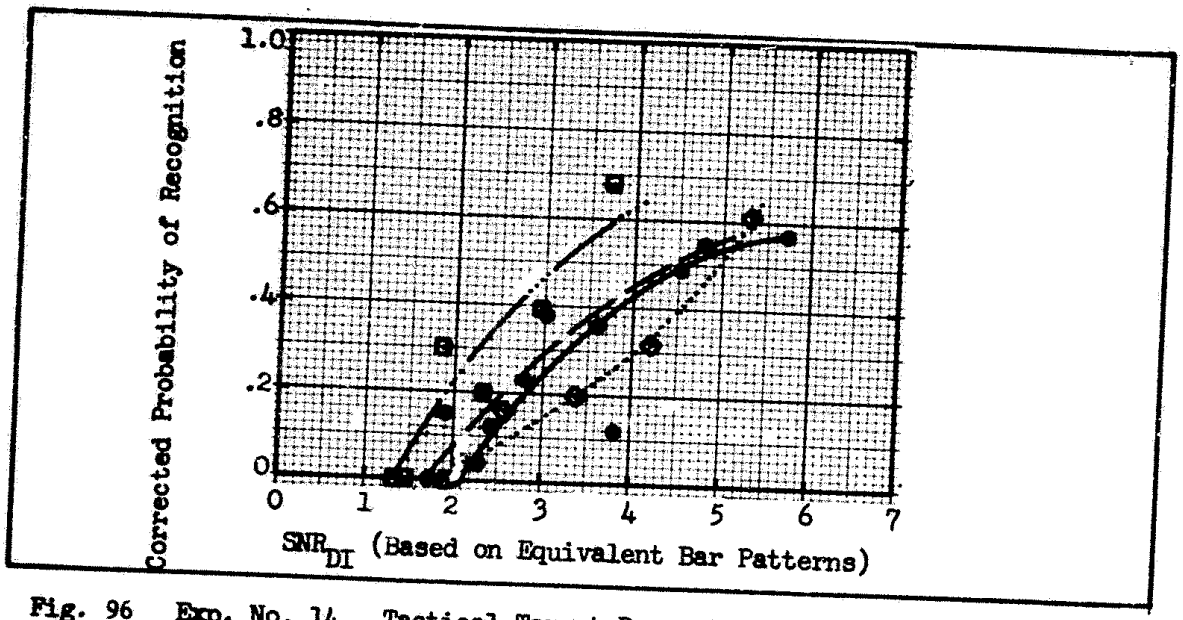

Fig. 96 Exp. No. 14. Tactical Target Recognition for Case C MTF
○ Tank, ● Derrick, □ Truck, ◇ Radar Truck

In Fig. 97 , we show the signal excursions for the tracked bulldozer on selected horizontal lines from the top to the bottom of the vehicle with line 1 being just above the object and line 17 just below. The MTF which was used was Case A. These traces were taken on every other line from a line selector oscilloscope. The dominant features of the bulldozer shown pictorially in Fig. 94 can be located in the traces of Fig. 97 . The boom arm is in traces 3 through 6, the cab in 6 through 8 and the bulldozer blade in 9 through 13. The boom appeared to be the most characteristic feature and the width was of the order of 1/8 width of the bulldozer.

Strictly speaking, the tactical targets are not either periodic or aperiodic in structure. However, as is discussed in the section on motion, if the aperiodic form of the SNR_{DI} equation is used together with the assumption that the original dimension, x_o, y_o can be associated with an

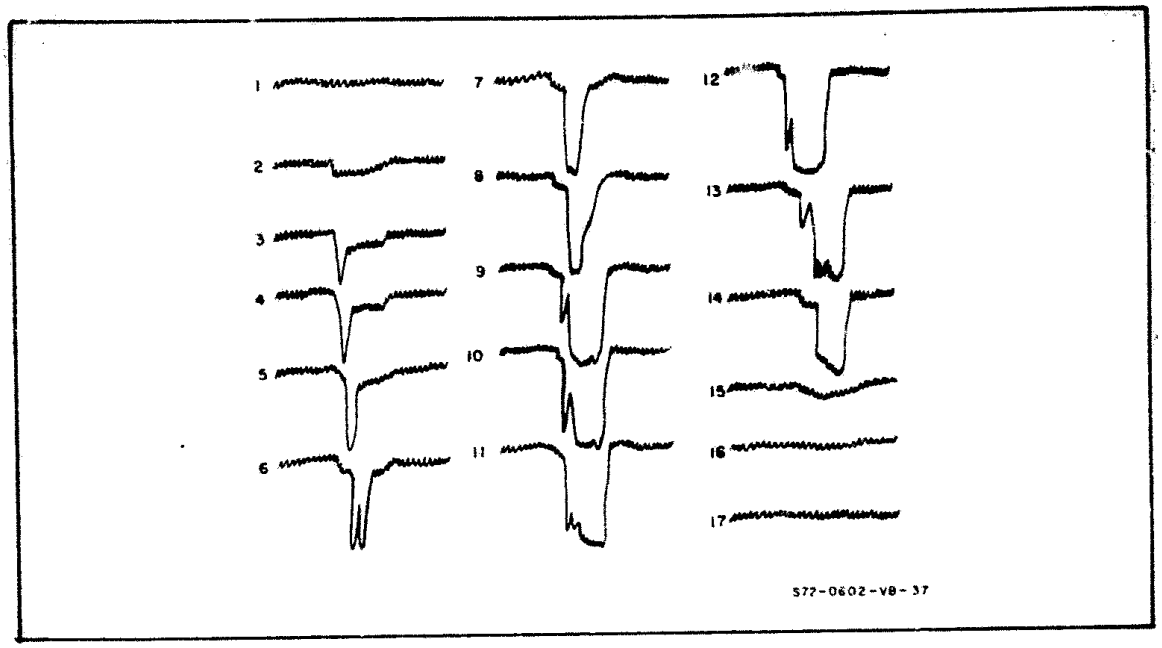

Fig. 97 Waveform of Derrick Half Track Along the Horizontal as a Function of Vertical Position of Scan Lines.

equivalent bar pattern (e.g. with bars y_o long and $x_o/8$ wide for recognition) then the static and motion results can be accounted for by the same threshold SNR_{DI} value. Furthermore, as we will now show, the same value SNR_D also holds for widely different MTF characteristics as well.

The value of aperiodic SNR_{DI} is calculated from

$$SNR_{DI} = \left[\frac{2t\Delta f_V x_o y_o}{\xi_{x_{LT}} \xi_{y_{LT}} 8A}\right]^{\frac{1}{2}} SNR_V \tag{167}$$

where

$$\xi_{x_{LT}} \xi_{y_{LT}} = \left[1 + \left(\frac{\delta_L}{x_o}\right)^2 + \left(\frac{\delta_T}{x_o}\right)^2\right]^{\frac{1}{2}} \left[1 + \left(\frac{\delta_L}{y_o}\right)^2 + \left(\frac{\delta_T}{y_o}\right)^2\right]^{\frac{1}{2}} \tag{168}$$

and

$$\delta_L = \frac{1}{N_{eL}} \tag{169}$$

$$\delta_T = \frac{1}{N_{eT}} \tag{170}$$

Using Eqs. (167), (168), (169), and (170), we have that for Case A $SNR_{DI} = 2.2$ whereas for Case C, $SNR_{DI} = 1.7$ and the two values of SNR_{DI} are somewhat closer in magnitude than those obtained ignoring MTF effects. The fact that the SNR_{DI} for poor MTF's is smaller may indicate that the effects of the poor MTF's are not quite as bad as the SNR_D equations would suggest. A similar result was obtained for bar patterns and we tentatively conclude that our theory is too pessimistic for very poor MTF's. Much more experimental data needs to be taken for different MTF cases to establish the limits of our theories.

6.0 Measures of Image Quality

There has been considerable interest by researchers in the optical and electro-optical field in finding a single measure of image quality. Such a number might be useful in comparing and specifying electro-optical components and may also be used in the design of the components. A specific design example is the shape of an MTF curve. In many cases, an MTF can be optimized for either a maximum low frequency response such as curve A of Fig. 98, or for a maximum high frequency response at the expense of the low frequency response as shown by curve B of the same figure. With the curve A, aperiodic signal levels will be generally higher than with curve B while with curve B, high frequency periodic patterns can be discerned that cannot be seen at all with an MTF corresponding to curve A.

To resolve fine image details, a sensor's MTF, projected into object space must be sufficiently high relative to the scene objects of interest. While a high MTF is a necessary condition, it is not sufficient. A fine grain photographic film may produce very high resolution of a day-lighted scene but be next to useless in a dimly lit cathedral. For the indoor scene, the photographer may need to select a coarser grain film of higher sensitivity. Similarly, a high resolution vidicon cannot compete with a moderately low resolution, low light level television at night but on the other hand, the high resolution vidicon camera will far outclass the LLLTV by day. It is thus readily evident that picture

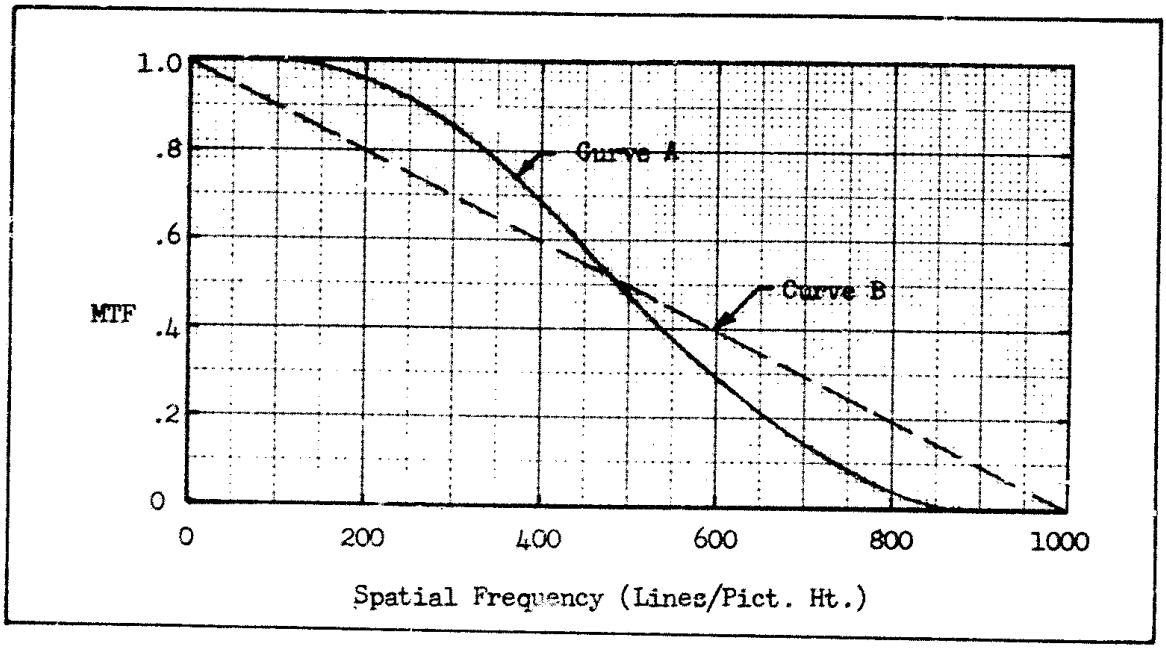

Fig. 98 Two Modulation Transfer Functions. Curve A Illustrates a High, Low Frequency Response While Curve B Illustrates a High, High Frequency Response.

quality is a function of both resolution limiting parameters such as the sensor MTF's and the sensor sensitivity. The picture quality can also be a function of the sensor's dynamic range and the scene itself.

To begin this discussion, we will first discuss the MTF related parameters and their effect on image quality. These factors have been the object of the most concern from a historical point of view.

6.1 MTF Related Image Quality Parameters

In 1881, Lord Rayleigh proposed a resolution measure for optical devices using two point source images. As discussed in Section 2, a lens images a point as a blur. As two point images are brought closer together, a point will be reached where they are no longer resolved as two points, but as one. Lord Rayleigh's criterion, however, demands

that the two images be resolved and the criteria was set so that the minimum signal excursion between the peaks of the two points and the valley between be 19% or more. This criterion is judged by many to be too severe, e.g., that the points can be resolved as two with a much smaller signal excursion. However, as we have noted above other factors must be considered. With test point images of low intensity, a 19% signal excursion may not be enough.

The modulation transfer curves such as those shown in Fig. 98 have been used in a similar manner. The "limit of resolution" has often been taken to be that spatial frequency at which the MTF has fallen to some low value such as 5% or 2%. The 2% figure is especially popular since it is often assumed that the eye cannot detect image contrasts below about 2%. However, image contrasts lower than 2% can be discerned by the unaided eye under many conditions. Also in many electro-optical sensors, the displayed contrast may be many times higher than the scene contrast. This is particularly true for FLIR equipments in the 8 - 13 μ band. With inherent scene contrasts of only a few percent, the displayed image contrast will usually be near 100%. Thus the eye's 2% "contrast limit" has little merit as a criterion when the displayed image contrast is varisble.

However, the modulation transfer function has a strong effect on picture quality. As we have shown in Sections 2 and 3, the modulation transfer function can both decrease perceived signal and increase perceived noise. It also limits the size of the smallest scene detail that can be seen. We note again before proceeding, that the smallest detail that can be seen is not only a function of the MTF but also of

the signal and noise levels and therefore a good sensor MTF alone does not guarantee high resolution. On the other hand, a high resolution of scene detail will not be obtained without a high MTF.

An MTF is synonymous with the frequency response of an electrical filter. As is well known, a wide frequency response is need to transmit short pulses and similarly a wide MTF is need to transmit point or line images. Electrical engineers are fond of the concept of equivalent bandwidth which is defined as the width of a rectangle whose area is the same as the area under the MTF curve. Since the value of the MTF at zero frequency is unity, the width of the rectangle (or equivalent bandwidth) is equal to

$$N_b = \int_o^\infty |R_o(N)|\, dN \quad . \tag{171}$$

Corresponding to N_b, there will be an equivalent impulse response width, δ_b, where

$$\delta_b = \frac{1}{N_b} \quad . \tag{172}$$

As is evident, the larger the bandwidth N_b, the smaller will be the equivalent impulse response width. Since the displayed image's detail is the convolution of the input image with the sensor's impulse response, a wide impulse response width will result in a loss of image detail.

The Eq. (171) can be written in two-dimensional form as

$$N_b(x,y) = \int_o^\infty \int_o^\infty |R_o(N_x N_y)|\; dN_x dN_y \quad . \tag{173}$$

This equation has been related directly to the Strehl measure of image

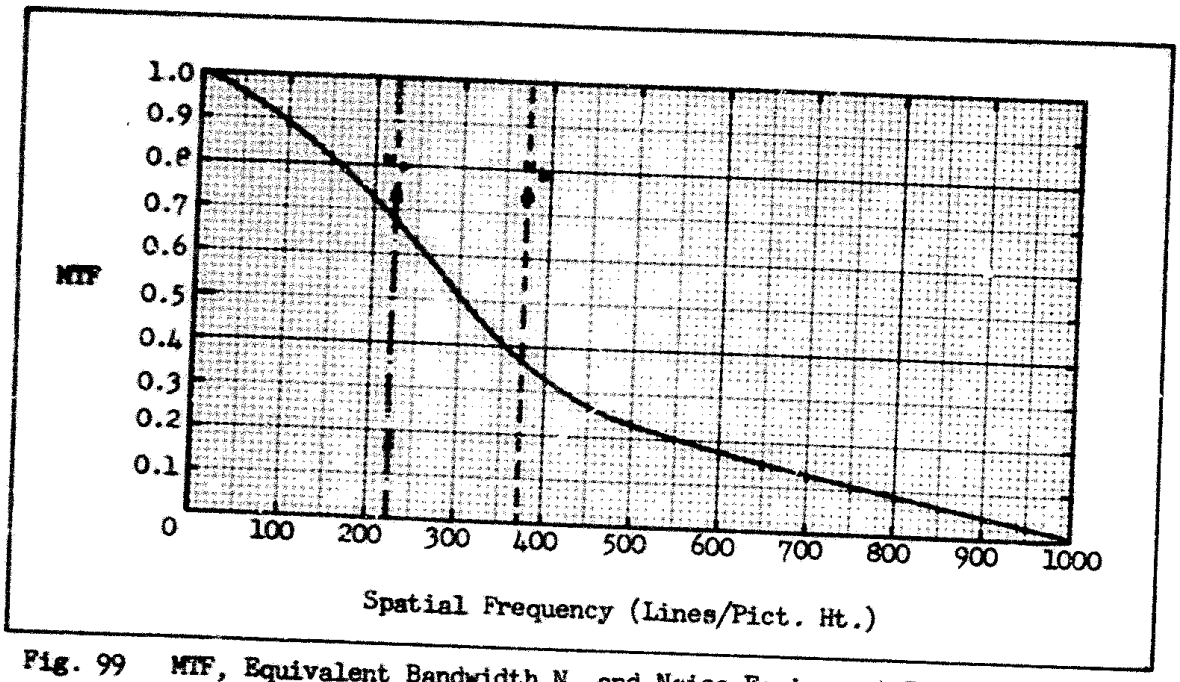

Fig. 99 MTF, Equivalent Bandwidth N_b and Noise Equivalent Bandwidth vs Spatial Frequency for a Typical 40/40/25 I-EBSICON Camera Tube.

quality (Ref. 9).

Schade (Ref. 9) has proposed the noise equivalent bandwidth, N_e, as a summary measure of quality where

$$N_e = \int_0^\infty |R_o(N)|^2 \, dN \quad . \tag{174}$$

Since $R_o(N)$ has a maximum value of one at zero frequency (for a linear system) and falls off with frequency, Schade's measure weighs the low frequency response more heavily than Eq. (171). The equivalent and noise equivalent bandwidths are shown for a typical MTF in Fig. 99.

Another figure of merit that has been extensively used is the acutance of an image (Ref. 10). The acutance is obtained in the following manner. A sensitive surface is partially covered with a knife

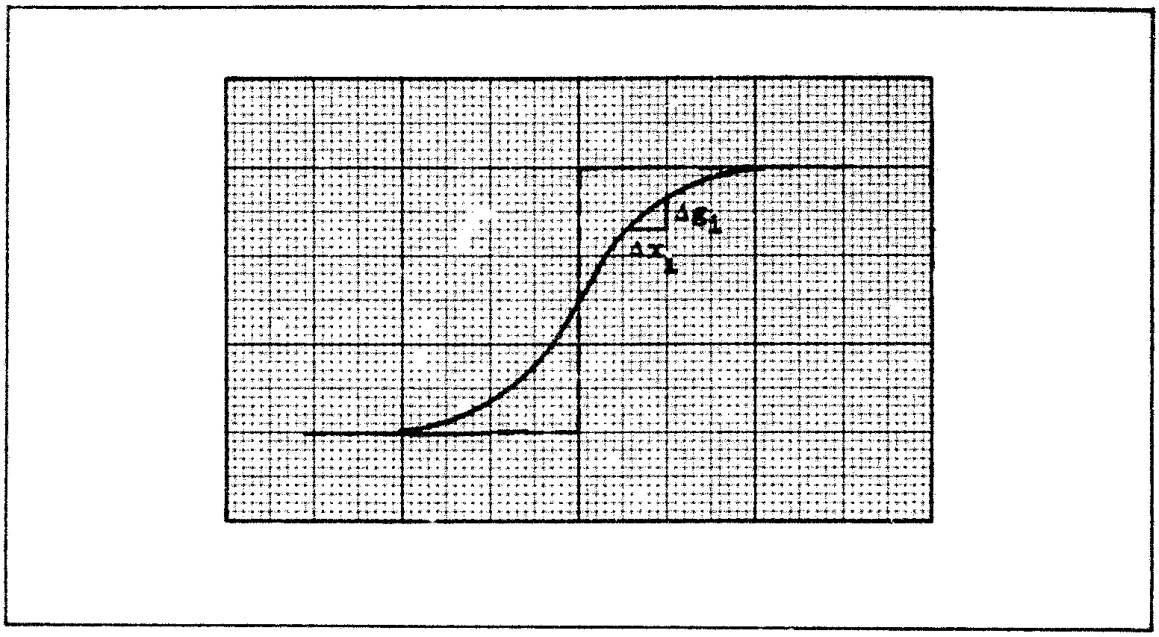

Fig. 100 Output Waveshape (———) for a Step Function Input (- - -). Slope of Output Waveshape, $\Delta g_i/\Delta x_i$ is used to Find Image Acutance.

edge and exposed to light. The light in the illuminated area does not stop at the knife edge but is diffused into the shielded region by reason of reflection, refraction, diffraction and scattering within the surface. Thus, the distribution of photoelectrons generated (or density of exposed grains in a photograph) instead being a step function assumes the typical S shape shown in Fig. 100. The slope of the S-shaped curve at any point is $\Delta g(x_i)/\Delta x_i$. The slope is determined for every position on the curve at equally spaced increments Δx_i and summed to give the expression

$$\bar{g}_x^{\,2} = \Sigma(\Delta g_i/\Delta x_i)^2/n \quad , \tag{175}$$

where n is the total number of Δx increments. The acutance is defined as

$$\text{Acutance} = \frac{\bar{g}_{x_i}^{\,2}}{I_s} \quad , \tag{176}$$

where I_s is the magnitude of the step in exposure. Acutance has been found to correlate with image sharpness.

Acutance bears a strong resemblance to Schade's N_e. The derivative of the unit step function $r_{-1}(x)$ is the impulse response $r_o(t)$, i.e.,

$$\begin{aligned} r_o(x) &= \frac{d}{d_x}\left[r_{-1}(x)\right] \\ &\sim \frac{\Delta r_{-1}(x_i)}{\Delta x_i} \end{aligned} \tag{177}$$

and

$$\begin{aligned} \Sigma \frac{\left[\Delta r_{-1}(x_i)\right]^2}{\Delta x_i} &\sim \frac{1}{nI_s} \Sigma \left(\frac{\Delta g_i}{\Delta x_i}\right)^2 \\ &\sim \int_{-\infty}^{\infty} r_o^{\,2}(x)dx \quad ; \end{aligned} \tag{178}$$

and by Parseval's theorem,

$$N_e = \int_o^{\infty} \left|R_o^{\,2}(N)\right| dN = \int_{-\infty}^{\infty} r_o^{\,2}(x)dx \tag{179}$$

as can be seen N_e is equivalent to, if not exactly the same as acutance.

Hufnagel (Ref. 9) evaluated 4 measures consisting of the one and two dimensional forms of N_e and N_b. He notes that none of

the functions meet his test for a measure "that is not invalid." (Hufnagel rates a measure "not invalid" if the objective vs subjective rankings of image quality plot as a rising straight line.) However, he claims the best results for the Strehl measure for photographs with substantially zero grain. For photographs with grain, he found a quantity Q_4^2 where

$$Q_4^2 = \frac{\iint_0^\infty |R_o(N_x N_y)| \, dN_x dN_y}{1 + \beta \iint_{00}^{\infty\infty} |R_o(N_x N_y)|^2 F(N_x N_y) dN_x dN_y} \tag{180}$$

which he dubs a grain modified Strehl measure. The above equation has the form of a signal-to-noise ratio for an aperiodic image.

Most of the work in defining picture quality measures has been performed using photographs. The usual procedure is to make photographs with lenses of different MTF's (but MTF's which are similar in shape). Observers are asked to grade the resulting pictures in order of "quality." It is not surprising that the pictures taken with the lenses of highest MTF proved to be the best or that the integral of the highest MTF (whether squared or not) has the largest numerical value.

A measure based on MTF alone applies only when the image, and the eye observing the image, is completely noiseless. Note also, that it may be necessary to include the observer's MTF in certain image quality determinations even if the noise is essentially negligible. However, no photoconversion process is completely noise-free and under many conditions, picture quality may be primarily limited by noise

rather than MTF. Indeed, much of the apparent lack of straight line correlation between image quality and a summary measure based on MTF alone may be due to the neglect of the noise.

In any event there is a growing belief that a summary measure of image quality must be based on signal-to-noise ratio and efforts in this direction are being made.

6.2 Signal-to-Noise Ratio Related Image Quality Parameters

As a first step in defining an image quality measure based on signal-to-noise ratio, Snyder (Ref. 9.) proposed that the measure be the integral of the display signal-to-noise above the observer's threshold (SNR_{DT}) as illustrated in Fig. 101. The solid curves represent the image signal-to-noise ratio obtainable from the sensor's display at two different light levels and the dashed curve represents the observer's threshold signal-to-noise ratio requirement. The area is that between a given solid line and the dashed line. Mathematically, the enclosed SNR_D area, called the MTF_A is given by

$$MTF_A = \int_o^\infty [SNR_D(N) - SNR_{DT}(N)]\, dN \quad . \tag{181}$$

SNR_D, for periodic bar patterns, is proportional to $R_{SF}(N)$ the square wave flux response and is inversely proportional to N, the spatial frequency, i.e.,

$$SNR_D \propto \frac{R_{SF}(N)}{N} \quad , \tag{182}$$

as N approaches zero, SNR_D approaches infinity. Even at low N, SNR_D

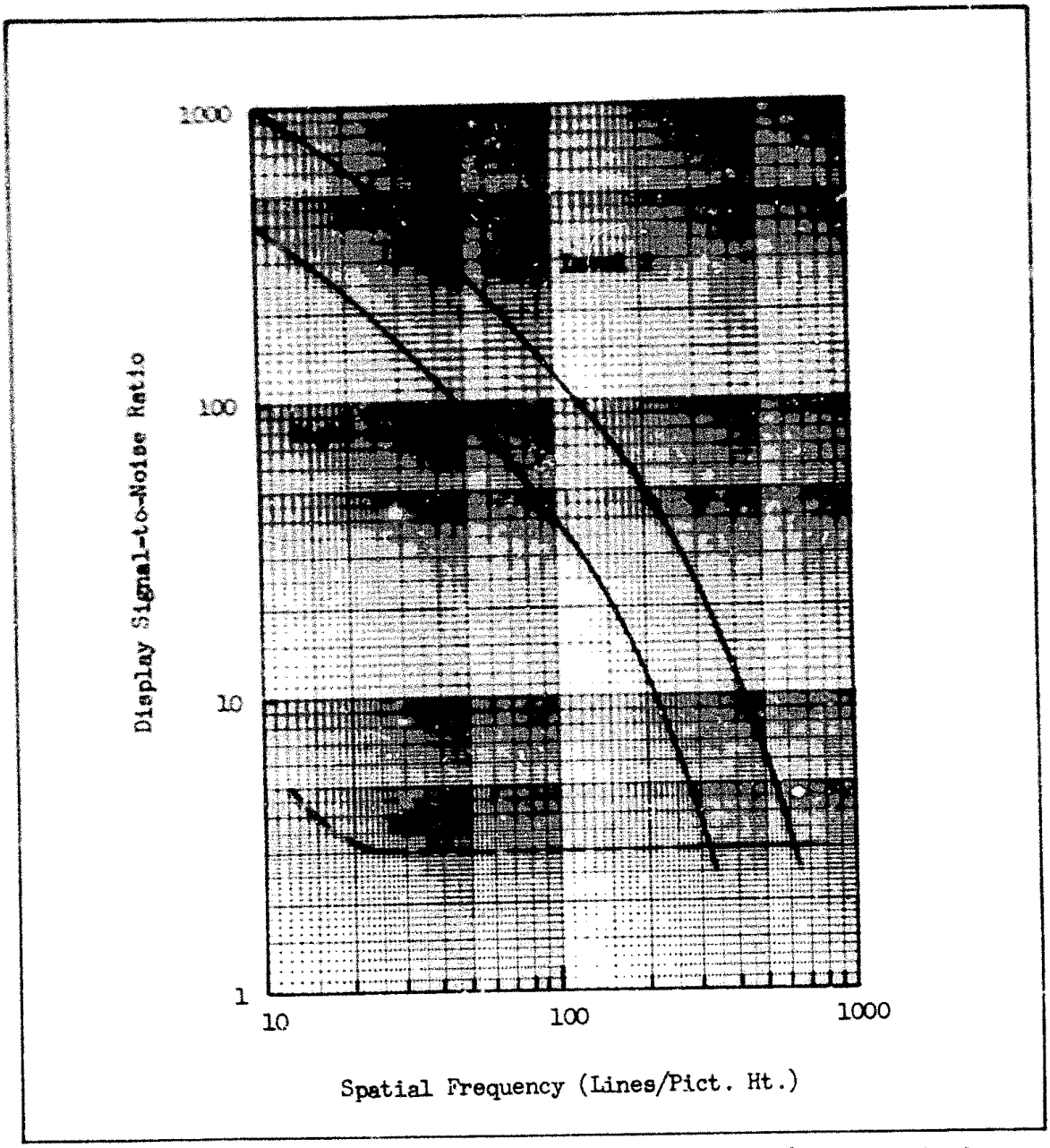

Fig. 101 Display Signal-to-Noise Ratio Obtainable (———) and Required (- - -) for Two Light Levels as a Function of Spatial Frequency.

becomes very large. However, the SNR_{DT} also increases at low spatial frequencies and thus integral of Eq. (181) should have a finite value. MTF is, of course, a function of the observer viewing distance since viewing distance influences the lowest spatial frequency observable.

MTF_A, generally weighs low spatial frequency response even more heavily than does N_e and the heavy weight of N_e on low frequency response has been one of the major criticisms of N_e. Schade (Ref. 4) also notes that MTF_A while generally a valid guide for systems with similar MTF's and noise characteristics is inappropriate for systems with dissimilar characteristics. In Schade's new measure, the balanced threshold resolution becomes the image quality criterion. By balanced resolution, Schade means the average of resolution calcaulated for periodic and aperiodic test patterns. Since periodic pattern detection weighs high spatial frequency response more heavily, the balanced resolution concept would presumably remove some of the heavy low spatial frequency response bias of N_e.

The goal of many researchers has been to find a single unitary measure of image quality. As we have shown, a single unitary measure is unlikely because of the dependence of image quality on image exposure and on noise. Rather than a single unitary measure, a function will result. It is agreed that the function should be based on image signal-to-noise ratio but that integral measures such as MTF_A may not result in the most useful form.

We currently favor the threshold resolution approach. An image quality measure such as MTF_A may show the relative "goodness" of two systems but the measure cannot be used to predict system performance in

the field. Threshold resolution incorporates all of the system parameters including image exposure time, light level, image stability, sensitivity, photoconversion noise, system generated noises, MTF and etc. Also, it can be used directly to estimate field performance — at least on a first cut basis. The previous complaint was that threshold resolution only applied to periodic bar patterns. The balanced resolution concept which has been discussed at some length in Section 2 circumvents this difficulty since it includes aperiodic objects. However, the method of weighing the aperiodic and periodic resolutions remain as an issue. We note that Schade's balanced resolution concept includes dynamic range (grey shades) which has not been included in the discussion of Section 2.

REFERENCES

1. Rosell, F. A., and Willson, R. H., "Performance Synthesis-Electro-Optical Sensors," Tech. Rept. No. AFAL-TR-71-137, Air Force Avionics Laboratory, WPAFB, Ohio, May 1971.

2. Rosell, F. A., and Willson, R. H., "Performance Synthesis-Electro-Optical Sensors," Tech. Rept. No. AFAL-TR-72-229, Air Force Avionics Laboratory, WPAFB, Ohio, August 1972.

3. Johnson, J., "Analysis of Image Forming System," Image Intensifier Symposium, Ft. Belvoir, Va., AD220 160, October 1958.

4. Schade, O. Sr., "Resolving Power Functions and Integrals of High Definition Television and Photographic Cameras--A New Concept of Image Evaluation," RCA Review, Vol. 32, December 1971.

5. Middleton, W. E. K., "Vision Through the Atmosphere," University of Toronto Press, Canada 1952.

6. Levi, L., "Motion Blurring with Decaying Detector Response," Applied Optics, Vol. 10, No. 1, Jan. 1971.

7. DeVries, H. L., Physica X, No. 7, July 1943.

8. Goodman, J. W., "Introduction to Fourier Optics," McGraw-Hill, 1968.

9. Biberman, et. al., "Preception of Displayed Information," Plenum Press, 1973.

10. Perrin, F. H., "Methods of Appraising Photographic Systems," Part 1, SMPTE, Vol. 69, March 1960.

UNCLASSIFIED

Security Classification

DOCUMENT CONTROL DATA - R&D

(Security classification of title, body of abstract and indexing annotation must be entered when the overall report is classified)

1 ORIGINATING ACTIVITY (Corporate author)
Westinghouse Defense and Space Center
Aerospace Division, Baltimore, Maryland

2a REPORT SECURITY CLASSIFICATION
Unclassified

2b GROUP
None

3 REPORT TITLE
Performance Synthesis of
Electro-Optical Sensors

4 DESCRIPTIVE NOTES (Type of report and inclusive dates)
Final Report

5 AUTHOR(S) (Last name, first name, initial)
Rosell, Frederick A.
Willson, Robert H.

6 REPORT DATE	7a TOTAL NO OF PAGES	7b NO OF REFS
July 1973	180	10

8a CONTRACT OR GRANT NO	9a ORIGINATOR'S REPORT NUMBER(S)
F33615-70C-1461	
b PROJECT NO: 698DF	
c	9b OTHER REPORT NO(S) (Any other numbers that may be assigned this report): AFAL-TR-73-260
d	

10 AVAILABILITY/LIMITATION NOTICES
Distribution limited to United States government agencies only; test and evaluation; 31 August 1973. Other requests for this document must be referred to Air Force Avionics Laboratory (NVA-698DF), Wright-Patterson Air Force Base, Ohio 45433.

11 SUPPLEMENTARY NOTES

12 SPONSORING MILITARY ACTIVITY
Air Force Avionics Laboratories
Wright-Patterson AFB, Ohio 45433

13 ABSTRACT

This effort is a continuation of the Performance Synthesis Study (Electro-Optical Sensors) reported in Technical Report AFAL-TR-72-229, dated August 1972. Analytical models were further developed and refined to include image motion and aperturing effects. Psychophysical experiments were performed as tests of the theories and it was found that the theory is reasonably accurate. A concept of balanced resolution is discussed which combines a system's performance for both aperiodic and periodic imagery. The question of a single figure of merit for a system is also discussed.

DD FORM 1 JAN 64 1473

UNCLASSIFIED

Security Classification

14. KEY WORDS	LINK A		LINK B		LINK C	
	ROLE	WT	ROLE	WT	ROLE	WT
Synthesis						
698DF						
Low-Light-Level Television						
Model						
Range						
Electro-Optics						
Sensors						
Video						
Perception						
Vision						
Signal-to-Noise Ratio Display						
Motion						
Apertures						